An image-based assay to quantify changes in proliferation and viability upon drug treatment in 3D microenvironments

Vasanth S. Murali[1,2], Bo-Jui Chang[1], Reto Fiolka[1], Gaudenz Danuser[1,2], Murat Can Cobanoglu[2], Erik S. Welf[1,2,*]

[1]Department of Cell Biology, UT Southwestern Medical Center, Dallas, TX

[2]Lyda Hill Department of Bioinformatics, UT Southwestern Medical Center, Dallas, TX

*Corresponding author; email: erik.welf@utsouthwestern.edu

Abstract

Every biological experiment requires a choice of throughput vs physiological relevance. Most primary drugs screens neglect for the sake of throughput critical parameters such as microenvironmental conditions, cell-cell heterogeneity, and specific readouts of cell fate. Here we develop a methodology to quantify proliferation and viability of single cells in 3D culture conditions, leveraging automated microscopy and image analysis to facilitate reliable and high-throughput measurements. The single cell resolution of this approach enables stratification of heterogeneous populations of cells into differentially responsive subtypes upon drug treatment. We detail experimental conditions that can be adjusted to increase either throughput or robustness of the assay. We demonstrate this approach by evaluating the effectiveness of a combination of RAF and MEK inhibitors on melanoma cells. We show that cells cultured in 3D collagen-based matrices are more sensitive than cells grown in 2D culture, and that cell proliferation is much more sensitive than cell viability. We also find that cells grown in 3D cultured spheroids exhibit equivalent sensitivity to single cells grown in 3D collagen, suggesting that for the case of melanoma, a 3D single cell model may be equally effective for drug identification as 3D spheroids models. We also illustrate the importance of measuring cell fates at the single cell level by showing heterogeneity in cell responses to drug treatment. Furthermore, we show that spheroids grown from single cells exhibit dramatic heterogeneity to drug response, suggesting a heritable drug resistance can arise stochastically in single cells but be retained by subsequent generations. In summary, image-based analysis renders cell fate detection robust, sensitive, and high-throughput, enabling cell fate evaluation of single cells in more complex microenvironmental conditions.

Introduction:

A fundamental paradigm in cell biological studies involves evaluation of cell responses to molecular perturbations. These perturbations typically leverage gene disruptions or pharmaceutical intervention to affect protein abundance or activity. Often, the responses to such perturbations are measured on cells subjected to *in vitro* conditions under the assumption that the observed phenotypes would translate to similar phenotypes *in vivo* [1, 2]. However, emerging evidence suggests that the three-dimensional characteristics of the cell microenvironment, including matrix dimensionality and stiffness, in part determine what phenotype will result from a certain perturbation [3-5]. As a result, cell biology researchers are increasingly turning towards three-dimensional assays to study cells in culture. Especially for pharmaceutical candidate screening, these assays are often considered too complex, expensive, or difficult to implement [6-8]. Unfortunately, this conclusion leads to a lack of data elucidating how perturbations affect cells under more complex conditions.

In addition to lacking microenvironment in drug screening studies, many high-throughput assays do not evaluate the effect of cell heterogeneity despite observations of drug resistance due to inherent or acquired heterogeneity in drug response [9-11] . For example, the difference between a compound that reduces proliferation in 100% of cells and a compound that kills 50% of cells, while leaving proliferation unaffected in the remaining cells, may result in dramatic clinical differences. Unfortunately, most drug screening assays employing measurements such as cell luminescence or enzymatic conversion activity as proxy measurements for cell number cannot discriminate between these situations [8]. Such measurements can yield imprecise results because reduced activity can mean there are fewer cells due to either decreased cell proliferation, increased cell death, or reduced cellular/metabolic activity. In order to evaluate drugs targeted for a specific purpose, assays must be capable of distinguishing these three effects in single cells, with the ultimate goal of integrating this capability into a high-throughput assay that is capable of discerning alternative cell fates at single cell resolution.

Here, we demonstrate the implementation of a simple, inexpensive approach for quantifying cell fates in response to drug treatment. Using this methodology, we evaluate the effects of drug treatment on cells cultured in 3D by analyzing its effect through cells in all the Z planes. We show the importance of matrix dimensionality and mechanics of the cell microenvironment by comparing melanoma cell responses under different experimental conditions during treatment with RAF/MEK inhibitor combination (RMIC) [12]. Our imaging-based assay can achieve relatively high throughput while maintaining single-cell resolution using automated microscopy and image analysis. Furthermore, we show that cytostatic and cytotoxic effects occur at different drug concentrations. We also show that the approach is amenable to evaluation of drug effects on a spheroid model. Surprisingly, we find that cells grown in spheroids exhibit very similar drug responses to single cells in a 3D microenvironment, in contrast to cells grown on 2D plastic plates. Therefore, we conclude that, at least under the conditions evaluated here, single cells in 3D microenvironments may be substituted for spheroid models of melanoma in order to dramatically increase assay throughput.

Results:

Measuring effects of drug treatment on cell proliferation and viability at single cell resolution

When designing an assay to quantify the effects of drug treatments, we identified three critical design criteria: (1) Single cell resolution, which enables identification of cell subtypes that respond differentially to treatment. (2) Ability to distinguish cytostatic from cytotoxic effects. (3) Ability to measure cell fates in complex 3D microenvironments.

We achieve these design goals by imaging and computational analysis of cells marked for proliferation and viability. Proliferation is measured by determining the cell area that is positive for newly synthesized DNA relative to a standard nuclear stain. Likewise, non-viable cells are identified either by disrupted membrane integrity (as indicated by ethidium homodimer in the nucleus) or intermediate apoptosis (as indicated by phosphatidyl serine on the outer leaflet of the plasma membrane) (Figure 1A). Multiple cell death markers are used to identify cells that may be in different stages of cell death due to the extended treatment time. Images are acquired throughout a thick 3D sample to create a 3D image stack, which is analyzed slice-by-slice and pixel counts summed to capture cell fate throughout the entire sample (Figure 1B).

Microenvironmental conditions affect melanoma cell sensitivity to RAF/MEK inhibition

To determine how environmental conditions affect cancer cell sensitivity to drug treatments, we compared the effects of RMIC on melanoma cells cultured on polystyrene tissue culture dishes to those cultured in a 3D collagen scaffold (Figure 1C). We chose collagen I for the scaffold because collagen I is the most abundant ECM protein in the human body [13, 14] and fills the majority of the interstitial spaces [15, 16]. ECM compositions that more closely mimic the basement membrane, such as those present in Matrigel, would be more appropriate for cells of epithelial origin.

We first tested our assay on A375 melanoma cell line, which harbors a BRaf V600E mutation that makes it a clinically-relevant recipient for the RMIC treatment, which targets the MAP kinase pathway by blocking RAF and MEK (Figure 1D). RMIC treatment for three days caused both a decrease in proliferation as well as a decrease in the fraction of viable cells, although the reduction in viability required a RMIC dose 10 times that required to elicit proliferation reduction (Figure 2).

Melanoma cells derived from two different melanoma patients that have been maintained as patient derived xenograft (PDX) models [17] also exhibited similar sensitivity to RMIC treatment in our assay. Cells from both PDX models exhibited proliferation reduction upon RMIC treatment, and cells from both patients were more sensitive to proliferation inhibition in 3D conditions than 2D conditions (Figure 3C and 3D). The effect on cell viability was more variable, however, as PDX 1 was sensitive to viability reduction regardless of the environmental condition (Figure 3A) but PDX2 exhibited only slight viability reduction at the highest drug concentration (Figure 3B). This result may be explained by the mutational status of PDX2, which expresses wild type (WT) BRaf, and thus is not expected to be sensitive to Dabrafenib, which only targets mutant BRaf. Overall, these results show that the 3D image-based assay enables precise measurement of different cell fates as a function of drug perturbations in 3D microenvironments.

Cell culture volume may be reduced to save reagents

Although cells cultured in 3D microenvironments are more sensitive to drug treatment, a disadvantage of the 3D culture system is the increased experimental cost. Thus, we sought to determine if smaller cell culture volumes may be employed to save reagents reduce costs and cell number requirements without suffering potential perturbations due to interactions of collagen with the tissue culture well [18, 19]. We observed no significant difference in effects of RMIC on proliferation or viability, although greater variability was observed in the 96 well data (Figure 4). This increased variability may be partially attributed to the apparent stiffness associated with the collagen near the walls of the multi-well dish, which is known to affect cancer cell fates [3, 20]. We conclude that 24 well or 96 well plates may be used for this assay, giving researchers the option of leveraging the cost savings and increased throughput offered by using 96 well plates at the cost of slightly increased variability compared to larger wells.

Flow cytometry is an effective alternative to imaging and computational analysis

Along with microscopy, flow cytometry is an alternative technique for measuring cell fate at single cell resolution, albeit without the spatial context and at the risk cell extraction and labeling may significantly distort the readout. We have adapted flow cytometric measurements to the assay described here by treating cells with RMIC and EdU in 3D collagen conditions exactly as for the imaging protocol, except the Click-iT reaction was performed in suspension according to the manufacturer's directions. This was done through the dissociation of collagen I using collagenase (Figure 5A). Cells positive for EdU staining were identified by gating a negative control group that was not incubated with EdU but Click-iT reaction performed (Figure 5B). Using this procedure, we find that flow cytometry and image-based analysis result in similar effects on proliferation as a function of RMIC (Figure 5C).

Imaging of low cell density suspension cells is an effective alternative to flow cytometry

Even for cell culture in suspension, image-based measurements are more robust than flow cytometry in situations where the harvestable cell numbers are low. In this case cells are labeled as for flow cytometry, but quantified by placing a drop of cell suspension on a microscope slide and covering the drop with a coverslip to force all cells into the same image plane (Figure 6A). When exposed to RMIC treatment, we observe that melanoma cells in suspension exhibit similar proliferation inhibition as cells in 3D collagen (Figure 6B and 6C).

Tumor spheroids exhibit drug sensitivity similar to single cells in 3D

Tumor spheroids are commonly used as 3D cell culture systems as they recapitulate several aspects of *in vivo* tumor morphology [6, 21, 22]. Here we use our cell fate measurement methodology to test the hypothesis that cells in 3D spheroids respond differently to drug treatment than single cells in a 3D microenvironment. Spheroids were formed by seeding cells in collagen at low density and culturing for 10 days before RMIC treatment. To rule out the possibility that wide field microscopy of the spheroids obscures cell fate measurements, we also performed light sheet fluorescence microscopy (LSFM), which limits the amount of out-of-focus light from the 3D sample by exciting fluorescence only in a thin sheet. Compared to epifluorescence imaging, LSFM produced images with individual nuclei that are much easier to distinguish (Figure 7A), improving our ability to identify cells that are marked for proliferation. However, this ability does not seem to affect our ability to measure proliferation in spheroids, as

samples imaged using LSFM show no significant difference in proliferation compared to samples imaged using epifluorescence microscopy (Figure 7B). This observation suggests that imaging by commonly available epifluorescence microscopy is sufficient to quantify cell fate, even for cells in complex environments such as spheroids. More surprisingly, cells treated with RMIC while they are in spheroids exhibited no significant difference in proliferation compared to single cells (Figure 7B). Hence, at least for the pathways tested here, drug effects can be tested in the much faster 3D single cell assay and do not require the growth of spheroids. It is also important to note that cells treated with RMIC under 2D conditions exhibited dramatically different proliferation than cells treated either as single cells in 3D or as spheroids. It remains to be determined which condition more faithfully reflects the response of cells to RMIC *in vivo*.

RAF/MEK drug resistance in spheroids shows heritability

While analyzing the 3D spheroid data, we noted for a few spheroids that proliferation continued despite RMIC treatment (Figure 7D). Because each spheroid corresponded to a clonal expansion of a single cell, this result suggests that some heritable drug resistance mechanism of the initiating cell was passed down to several generations of daughter cells. We also noted that several spheroids possess only one or two proliferative cells, suggesting that drug resistance is either stochastically heritable or transient. Indeed, a recent study on melanoma resistance to a Braf inhibitor suggests a transient resistance mechanism [10], although it is not known if the transiently resistant cells studied by Shaffer *et al.* would also be resistant to the RAF/MEK inhibitor combination studied here.

Discussion

In order to streamline drug discovery, we must develop methods to evaluate compound efficacy under increasingly complex extracellular microenvironments [23, 24]. However, experimental complexity must be balanced with throughput, cost, reproducibility, and precision. Here, we describe an assay that enables high-throughput compound evaluation without sacrificing single cell resolution, readout specificity, or microenvironmental complexity. Indeed, although we evaluated this assay using 3D collagen scaffolds, it is equally amenable to other scaffolds and would be equally useful for identifying which ECM components affect drug efficacy. Our results show that even a simple 3D collagen microenvironment affects how cells respond to treatment, rendering melanoma cells more sensitive to treatment under 3D conditions compared to 2D conditions. This observation suggests that many potentially useful compounds might have been ignored because they were tested on cells under 2D conditions. The work presented here removes the barriers to measuring perturbations in more realistic microenvironments by providing a resource for sensitive, high-throughput, cost-effective compound evaluation.

In addition to facilitating study of more complex microenvironments, a key feature of the presented methodology is the ability to measure single cell responses. Conventional methods of evaluating 3D cell culture assays involve chemiluminescence or enzymatic conversion that yield high throughput results but at the cost of losing single cell resolution [25-27]. Alternatively 3D cultures may be imaged to detect responses at the single cell resolution but such an approach requires complex image analysis protocols to convert high resolution images into quantitative results[28, 29]. In this work, we employed the freely available and popular CellProfiler image analysis package to evaluate data throughout a 3D image stack. We anticipate that the combination of automated image acquisition on a relatively low cost microscope

combined with freely available analysis software will encourage application of this approach in various laboratory settings.

The ability to discriminate cytotoxic from cytostatic compounds and as a result identify more sensitive cell fate readouts will also streamline drug discovery. For example, we show that although the RAF/MEK inhibitor combination rapidly inhibits proliferation of both a melanoma cell line and two different melanoma PDX-derived cell models, it has variable effects on cell viability. These results suggest that although this treatment may be effective at slowing tumor growth, it would ultimately be more effective if combined with a more specific cytotoxic therapy. Thus, it is our hope that more sensitive, more precise measures of cell fate will enable more accurate predictions of *in vivo* efficacy that will render drug discovery and optimization more effective.

We have employed this assay to test the hypothesis that melanoma spheroids offer a more realistic paradigm for drug evaluation than 2D cultures. This is indeed the case – A375 cells grown in spheroids are more sensitive to proliferation inhibition than cells grown on plastic dishes. However, we observe that cells grown as single cells in 3D are equally sensitive to RMIC when compared to cells grown in spheroids. While this behavior remains to be tested on a system-by-system basis, this outcome greatly reduces the time necessary to grow spheroids without sacrificing assay sensitivity.

Materials and Methods:

Tissue culture materials

A375 melanoma cells harboring the BRaf V600E mutation were purchased from ATCC (CRL-1619). DMEM with high glucose and L-glutamine was purchased from Gibco (11965-167). A375 cells were cultured in DMEM supplemented with 10% fetal bovine serum (FBS). Two PDX cell models PDX1 and PDX2 were acquired from the University of Michigan via Sean Morrison at UT Southwestern Medical Center. PDX1, like A375, is a BRaf V600E mutant melanoma cell line and PDX2 is a BRaf WT melanoma cell line. Both PDX1 and PDX2 primary cells were cultured in Dermal Basal Medium purchased from ATCC (PCS-200-030), supplemented with adult melanocyte growth kit purchased from ATCC (PCS-200-042), which includes rh insulin, ascorbic acid, L-Glutamine, epinephrine, $CaCl_2$, peptide growth factor and M8 supplement. Trypsin/EDTA was purchased from Thermo Fisher (R001100). For 3D culture, collagen I was purchased from Advanced Biomatrix (5005-100). Dabrafenib (Dab), a BRaf V600-targeting inhibitor (GSK2118436), and Trametinib (Tram), a potent MEK1/2 inhibitor (GSK1120212) were purchased from Selleckchem. Ethidium homodimer, a cell impermeant viability marker, was purchased from molecular probes (E1169). Apopxin, a phosphatidylserine sensor, was purchased from ABCAM (ab176749). Hoechst 33342 nuclear stain was purchased from molecular probes (H3570). Click-iT based imaging kit (C10340) and flow cytometry kit (C10632) were purchased from molecular probes. Phenol red free DMEM with high glucose and L-glutamine for fluorescence imaging was purchased from Gibco (21063-045). The phenol red free media was supplemented with 10% FBS. Hanks balanced salt solution (HBSS) with no calcium or magnesium was purchased from Gibco (14170112). Collagenase Type I powder to breakdown collagen was purchased from Gibco (17100017). Tetrafluoroethylene perfluoropropylene (FEP) tubes for spheroid light sheet imaging were purchased from BOLA, Germany (1815-04).

2D cell culture

All 2D cell cultures were performed in 24 or 96 well plates. Cells at ~70% confluency were washed in 1X PBS, trypsinized, and harvested at 500 g for 5 min. The cell pellet was then resuspended in 1-5 mL media depending on the cell density. The concentration of cells was determined using a cell counter and the dilution was adjusted to 200µL per well for 96 well and 500µL per well for 24 well plates. The cells were seeded at a final density of 15,000 cells/well for 24 well and 5,000 cells/well for 96 well plates. The cells were incubated overnight to allow them to attach to the bottom of the dish. For drug evaluation in 2D, a 10mM stock drug concentration was prepared in DMSO. A 2X desired concentration of the drug was first prepared in media. This was followed by a 1:1 dilution in media, which yielded the desired final concentration. Controls received the same amount of vehicle (DMSO) as the drug treated cells. The cells with drug were then incubated for the desired time, and 24h prior to analyzing the results EdU was added. A 20µM EdU solution was mixed with 2X drug and diluted 1:1 with media to give a final concentration of 10µM EdU and was incubated with the cells for 24h.

3D cultured single cell culture and spheroids

All 3D cell culture experiments were performed in 24 or 96 well plates. 10X PBS, 1M NaOH and water were pre-warmed in a 37°C water-bath. The multi well plate was pre-warmed in 37°C incubator and an aliquot of 3mg/mL collagen was brought to room temperature. Cold reagents can lengthen the collagen polymerization time, resulting in cell settling at the bottom of the dish, which does not recapitulate the 3D morphology. The cells were trypsinized, harvested and resuspended in 1-5 mL media depending on the cell density. The concentration of cells was determined using a cell counter and the desired volume of cells were centrifuged to acquire a pellet with the desired cell number. The pellet was resuspended in 2mg/mL collagen. To prepare collagen at a final concentration of 2mg/mL from 3.2mg/mL stock, we combined 100µL 10X PBS, 10µL 1M NaOH, 250µL water and 640µL of 3.1 mg/mL collagen stock. The pH was measured to be between 7-7.4 using pH strips. The cell pellet was resuspended in 2mg/mL collagen and added to the pre-warmed multi-well plate. The cells were incubated for 30 min in 37°C incubator. Collagen polymerization was observed through change in color of the solution from a transparent solution to an cloudy gel. Media was then added to cells and incubated overnight. For RMIC evaluation in 3D, drug dilution was performed as described above for 2D cell culture.

A375 melanoma spheroids were created in 3D collagen by suspending single cells in collagen and culturing them over 10 days with frequent replacement of media to form 3D cultured spheroids.

RMIC treatment as a function of concentration in 2D and 3D

A375, PDX1 and PDX2 melanoma cells were setup in multi-well plates in 3D collagen and 2D culture platforms. To determine the effect of concentration in 3D and 2D cell culture platforms, the cells were incubated with RMIC at 10nM Dab+1nM Tram, 100nM Dab+10nM Tram and 1µM Dab+100nM Tram with a DMSO control. The DMSO and RMIC treated cells were incubated for 3 days as a function of concentration. Forty-eight hours post incubation with RMIC, 10µM EdU was added to cells along with the desired DMSO and RMIC concentration and cells were incubated for an additional 24h for a total of 3 days incubation with RMIC.

Viability imaging in 2D and 3D

Following treatment with RMIC, the cells were tested for viability as a function of concentration and time. The drug treated media was aspirated from the cells and incubated with 4µM ethidium homodimer, 2µL Apopxin per 100µL media and 15µg/mL Hoechst 33342 in phenol red free medium supplemented with 10% FBS. The cells were incubated with fluorescent reagents for 30 min. Following incubation, imaging was performed with a Nikon *Ti* epifluorescence microscope with an OKO temperature and CO_2 control system regulated at 37°C with 5% CO_2. The cells in 3D were imaged with a z-step size of 2.5µM and a total of 201 steps. Following image acquisition, the cells were prepared for Click-iT EdU imaging to determine cell proliferation.

Proliferation imaging with Click-iT EdU in 2D and 3D

To identify cells undergoing S phase, cells were incubated with modified thymidine analogue EdU for 24 hours and labeled using click chemistry. Following viability imaging, the cells in 2D and 3D were washed with 1X PBS. Following washing, the cells cultured in 3D were fixed with 4% paraformaldehyde for 30 min at 37°C, and the cells in 2D were fixed for 20 min at room temperature. The fixed cells were permeabilized with 0.5% Triton X-100 for 30 min in 3D and 20 min in 2D. Note that the 0.5% Triton X-100 was prepared from a 25% stock solution. The 25% stock should be stored at 4°C and diluted to 0.5% before use. The Click-iT reaction was then performed using the Click-iT EdU assay imaging kit with Alexa Fluor 647 fluorophore. The Click-iT reaction was partially modified from the manufacturer's protocol such that the Alexa Fluor 647 azide was first diluted 1:100 in DMSO before adding the amount specified by the manufacturer's protocol was then added. This dilution needs to be modified based on cell type. If the Alexa Fluor 647 is used directly as per manufacturer's protocol in 3D the dye will non-specifically bind to the collagen, creating a high background.

Image analysis using Cell Profiler and data processing

To analyze all the 2D and 3D images it was important to identify software that can be used with minimal computational experience. We identified Cell Profiler as an ideal candidate (Carpenter, et al., 2006; Kamentsky, et al., 2011) (http://cellprofiler.org). We used Cell Profiler V 2.2. To operate Cell Profiler we established image analysis pipelines that can accept our multi-point z-stack images and analyzed data for positive pixels from each channel.

The z-stack images were acquired as individual TIFF files. A distinguishing parameter such as a unique name for each channel was used while acquiring 3D and 2D images. In the input module under "NamesAndTypes" we defined the distinguishing name for each channel to help the software separate images from different channels. We used a robust background thresholding method to distinguish foreground (i.e. marked cells) and background regions. The pixel areas of foreground regions were measured for each channel.

While using two dead cell markers (apopxin and ethidium homodimer) to identify different phases of cell death, we observed some cells that were marked by both dead cell markers. To identify cells that were counted twice we created a mask to identify overlapping regions and then subtract that area so they are counted only once. For analyzing the cell proliferation data the pipeline was modified to two channels and the mask function was removed. Both the viability and proliferation data was exported for further quantification to a spreadsheet.

To analyze the viability data we first subtracted the overlapping pixel area of the dead cell channels (apopxin and ethidium homodimer) from the total area of the dead cells channels. A log (ratio+1) of the total pixels from hoechst to the dead cell pixels was calculated and averaged over all images acquired for a particular treatment. The average values for each treatment were normalized to the DMSO control; and these values were referred to as viability scores. Analogously, proliferation scores were computed based on averaging and normalization of the log (ratio+1) of the total pixels from Hoechst to EdU pixels.

Evaluating effect of well size by comparing viability and proliferation in 24 and 96 well plates

The effect of RMIC on viability and proliferation as a function of concentration in A375 cells was evaluated in 24 well plates. We evaluated similar experimental conditions in a 96 well plate to compare results to that of 24 well plates. A375 cells were plated in 2 mg/mL collagen in 3D. The cells were then treated with RMIC as a function of concentration for 3 days. On day 2 of RMIC treatment, 10µM EdU was added for an additional 24h. After 3 days total incubation, viability and proliferation assays were performed as described above.

Comparing imaging and flow cytometry for RMIC as a function of concentration

To validate the robustness of the 3D imaging platform, we measured RMIC effect on proliferation using the flow cytometry as an independent method. A375 cells were incubated with drugs as a function of concentration. The cells were incubated with drugs for 3 days and on day 2 of treatment, EdU at a final concentration of 10µM was added to the cells. Following incubation with RMIC and EDU, the collagen was washed with Hanks balanced salt solution (HBSS). The collagen was then treated with collagenase as per manufacturer's protocol for 30 min at 37°C to breakdown the collagen completely. Media with 10% FBS was then added to neutralize the effect of collagenase.

A flow cytometry based Click-iT reaction was performed as per manufacturer's protocol. In brief, the cells were centrifuged to collect the pellet. The pellet was resuspended in 4% PFA for fixation and permeabilized with 1X Tween-20. The Click-iT reaction was performed and the flow cytometry was gated using a negative control where the cells were not treated with EDU. To analyze the results, a uniform gating was setup by using the FlowJo software with a baseline negative control. The treated samples were the gated under the same settings.

Imaging cells in suspension using the Click-iT flow cytometry kit

Since the Click-iT EdU based imaging kit was designed for adherent cells, we aimed to design an imaging based method to determine proliferation for cells in suspension. We thus tested the application to imaging of a flow cytometry kit that is designed for suspended cells. To do so we cultured A375 melanoma cells in low adhesion 6 well plates. The cells were then treated with RMIC at 10nM Dab+1nM Tram and 1µM Dab+100nM Tram for 3 days. On day 2 of RMIC treatment, 10µM EdU was added for an additional 24h. After 3 day incubation with RMIC, Click-iT reaction was performed with the flow cytometry kit as per manufacturer's protocol. The cells were also stained with Hoechst for imaging purposes. A drop of the cell suspension after the Click-iT reaction and Hoechst treatment was put on a glass slide and images were acquired on the Nikon *Ti* microscope. The cell images for nuclei Hoechst staining and EDU proliferation were analyzed on Cell Profiler.

Melanoma spheroid preparation for light sheet fluorescence microscopy (LSFM)

Tumor cell spheroids were created from single melanoma cells by culturing cells in sample holders as described here. FEP tubes were cut into small pieces with holes made along the walls using a 27G needle in order to allow media exchange across the tube. The tubes were cleaned with 30% bleach for 30 minutes and placed in 100% EtOH overnight. The sterile tubes were dried and pre-warmed in a 37°C incubator. A375 melanoma cells were prepared in 3D collagen as described above and seeded at low density within the FEP tubes. The collagen was allowed to polymerize at 37°C, fresh media was added, and then the cells were incubated for 10 days with regular replacement of media. The spheroids then underwent RMIC treatment for 3 days with 24h EdU incubation. Following RMIC treatment and EdU incubation, the Click-iT imaging assay was performed and the spheroids were imaged on the LSFM.

To image spheroids, a low magnification LSFM was constructed with a large field of view. To increase the field of view, and improve optical penetration, a conventional dual illumination LSFM was built that permits scanning of the beam in the Z-dimension as well as pivoting the light-sheet in the sample plane to reduce shadowing and stripe artifacts [30]. For illumination, four lasers (405nm, 488nm, 561nm, and 640nm, Coherent, OBIS) are combined with dichroic mirrors (MUX Series, Semrock), spatially filtered and expanded with a telescope consisting of an achromatic convex lens (f=50 mm, Thorlabs, AC254-050-A-ML), a pinhole (100 µm, Thorlabs, P100H), and an achromatic convex lens (f=400 mm, Thorlabs, AC254-400-A). An achromatic Galilean beam expander (Thorlabs, GBE02-A) further increases the laser diameter by 2x. All solid-state lasers are directly modulated with analog signals originating from a field-programmable gate array (PCIe-7252R, National Instruments) that have been conditioned with a scaling amplifier (SIM983 and SIM900, Stanford Research Systems).

For light-sheet generation, a cylindrical lens (f=50 mm, Thorlabs, ACY254-050-A) is used to focus the laser illumination into a sheet, which is relayed to the illumination objective (Nikon 10X Plan Fluorite, NA 0.3) with two mirror galvanometers (Thorlabs, GVS001), two coupling lenses (f=50 mm, Thorlabs, AC254-050-A), and a tube lens (f=200 mm, Thorlabs, ITL-200). The Z-galvanometer is conjugate to the back pupil of the illumination objective, whereas the pivot galvanometer is conjugate to the sample. To generate the second illumination arm of the microscope, a polarizing beam splitter (Newport, 10FC16PB.3) is placed after the second coupling lens, and two lenses (f=200 mm, Thorlabs, AC508-200-A) relay the scanned illumination to a second tube lens and illumination objective. Because the counter-propagating light-sheets are orthogonally polarized, there is no interference from the two light-sheets, and a half-wave plate (AHWP10M-600) placed in front of the polarizing beam splitters is used to adjust the intensity of the two light-sheets. To control the light-sheet thickness, a variable slit was placed in the back-pupil plane of the cylindrical lens, which is conjugated to the back-pupil planes of both illumination objectives.

For detection, a 16x, NA 0.8 objective lens (Nikon CFI75 LWD 16X W) and a tube lens (f=200 mm, Edmund optics, 58-520) form the image on a sCMOS camera (Hamamatsu, C11440, ORCA-Flash4.0). A laser line filter (Chroma, ZET405/488/561/640) is placed after the detection objective lens and a filter wheel (Sutter Instrument, Lambda 10-B) equipped with multiple bandpass filters is placed between the tube lens and the camera. The detection objective lens is mounted on a piezo-driven stage (Mad-City Labs, Nano-F450) that provides 450 µm travel range. The sample stage is a combination of a three-axis motorized stage (Sutter Instrument, MP285) and a rotation stage (Physik Instrumente, U-651.03). The microscope is controlled by custom-written LabVIEW software (Coleman Technologies, National Instruments).

Acknowledgements

This research was funded by grants from the National Institutes of Health (K25CA204526 to ESW), the Cancer Prevention Institute of Texas to (R1225 to GD and RR160057 to RF) and Lyda Hill Department of Bioinformatics startup funds to MCC. We would like to thank Andrew D. Jamieson for help in building Cell Profiler pipelines, Heather Grossman for cell sorting, Sean Morrison for PDX-derived cell models, Xuexia Jiang for help with file conversions and Meghan Driscoll, Etai Sapoznik and Maralice Conacci-Sorrell for providing valuable feedback on the manuscript.

Author Contributions

V.S.M. and E.S.W. conceived the project. G.D. and M.C.C. provided intellectual input. V.S.M. and E.S.W. made the figures. V.S.M. designed and performed the experiments. B.J.C. and R.F. constructed the LSFM. V.S.M., B.J.C., R.F., G.D., M.C.C., and E.S.W. wrote the manuscript.

Competing Interests

The authors declare no competing interests.

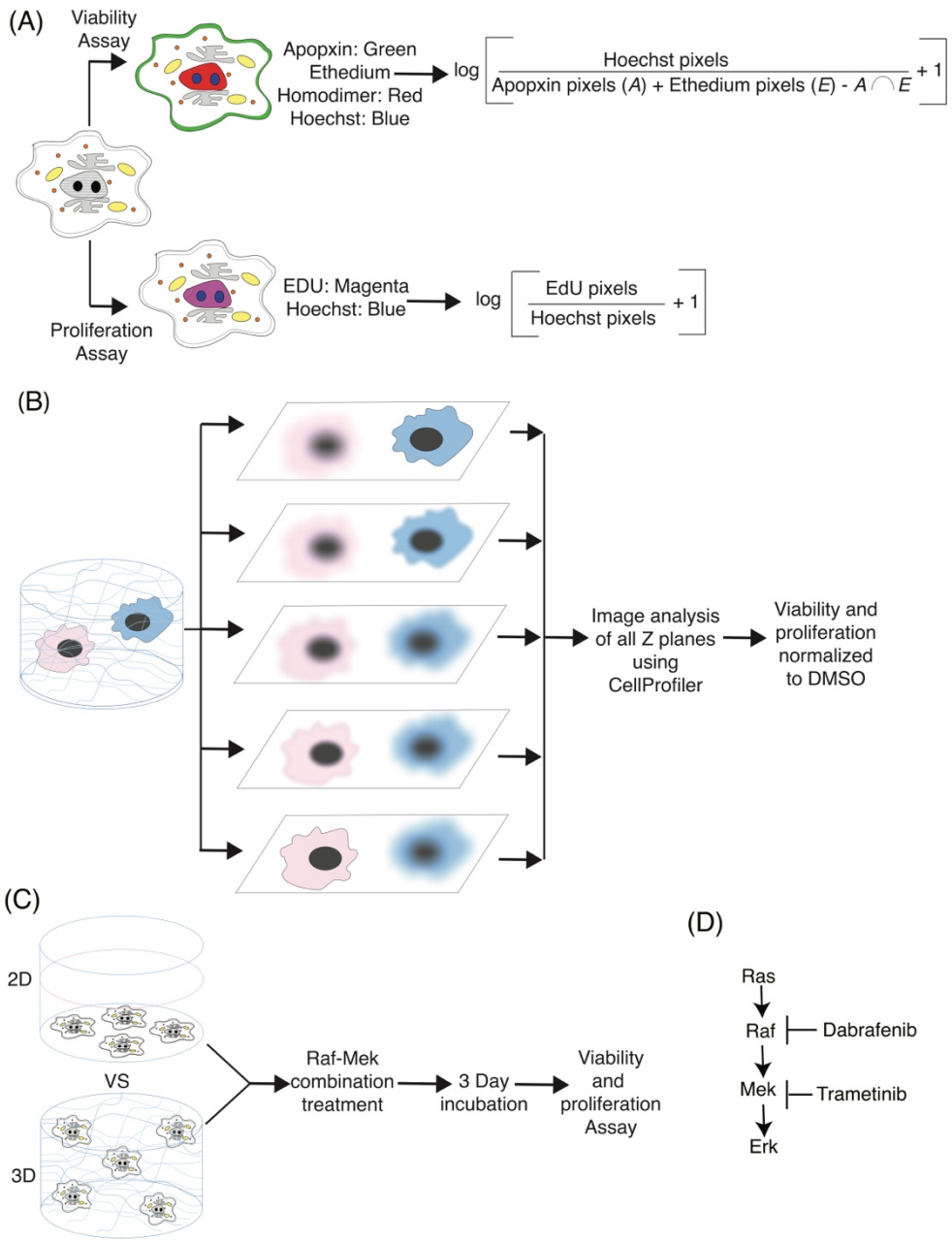

Figure 1: Image-based proliferation and viability measurement in 2D and 3D samples. (A) Cell viability is measured by image-based quantification of cells positive for extracellular phosphatidyl serine (apopxin) or disrupted plasma membrane (ethidium homodimer) and proliferation is measured by image-based quantification of cells positive for EdU incorporation over a 24 hour period. **(B)**. Quantification in 3D samples is performed by obtaining a 3D image stack, analyzing each image slice separately using CellProfiler, and aggregating data from all image slices. **(C)** To compare the effects of the microenvironment on drug efficacy, drug effects on melanoma cells cultured in standard 2D polystyrene dishes were compared with cells cultured in 3D collagen. (D) RMIC treatment targets the Raf and Mek in the MAP kinase pathway.

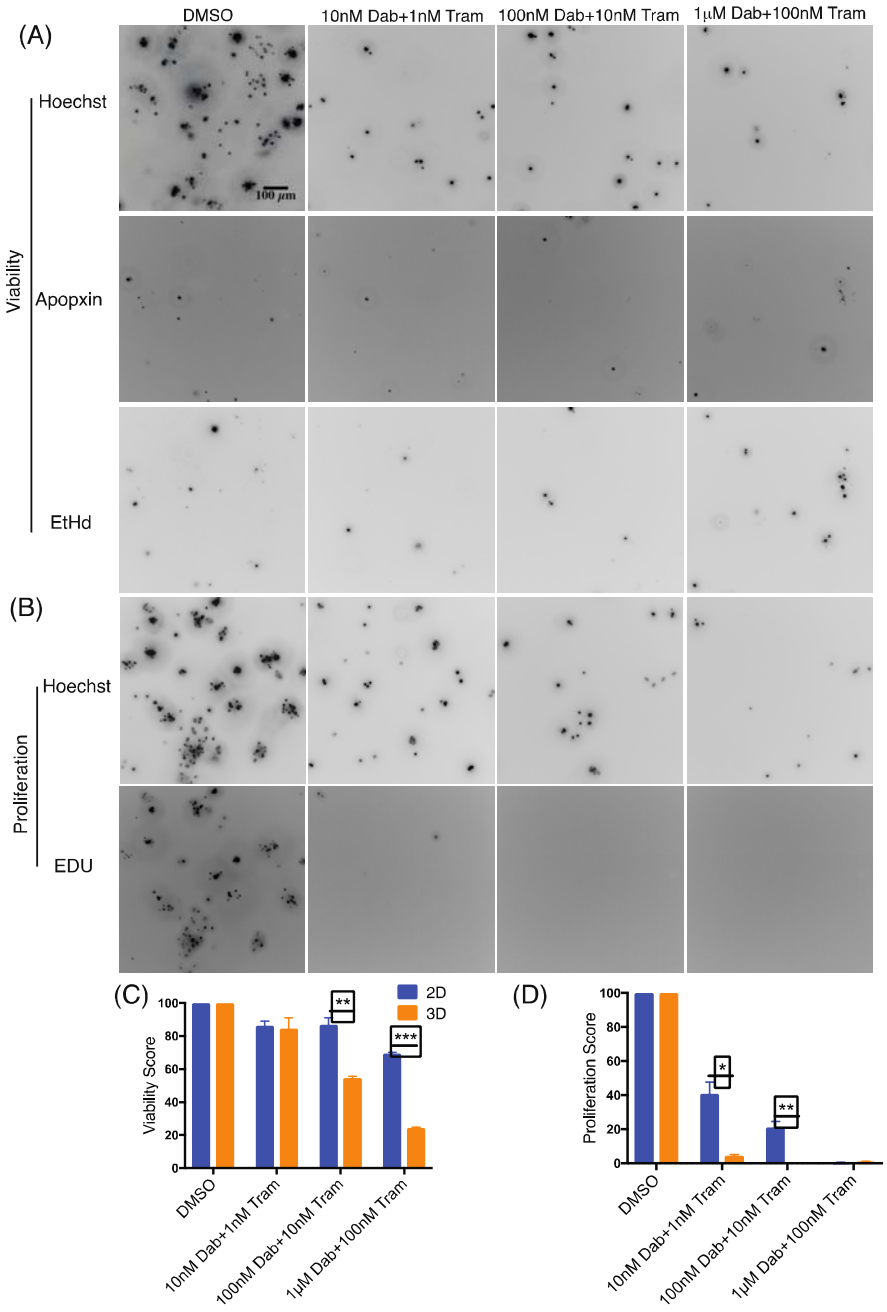

Figure 2: Cell fate assay reveals differential sensitivity of proliferation and viability in 2D and 3D microenvironments. Example images show maximum intensity projections of 3D Z-stacks of A375 cells stained with viability markers (A) and a proliferation marker (B) cultured in 3D collagen and treated with various concentrations of the Raf/MEK inhibitor combination. Aggregate proliferation (C) and viability scores (D), normalized to DMSO controls, for A375 cells cultured either in 2D dishes or 3D collagen cultures are shown for three independent experimental repeats with results presented as average ± SEM (*$p < 0.005$, ** $p < 0.0005$, *** $p < 0.00005$).

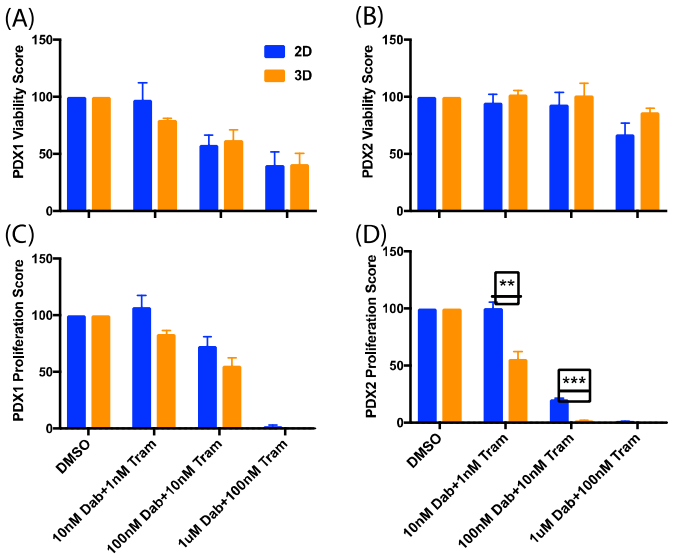

Figure 3: Cells from PDX tumors are more sensitive to proliferation inhibition in 3D microenvironments than 2D. Aggregate viability (A & B) and proliferation (C & D) scores for PDX1, a BRaf V600E mutant melanoma, and PDX2, a BRaf WT melanoma, normalized to DMSO controls, cultured either in 2D dishes or 3D collagen cultures are shown for three independent experimental repeats with results presented as average ± SEM (** $p < 0.0005$, *** $p < 0.00005$).

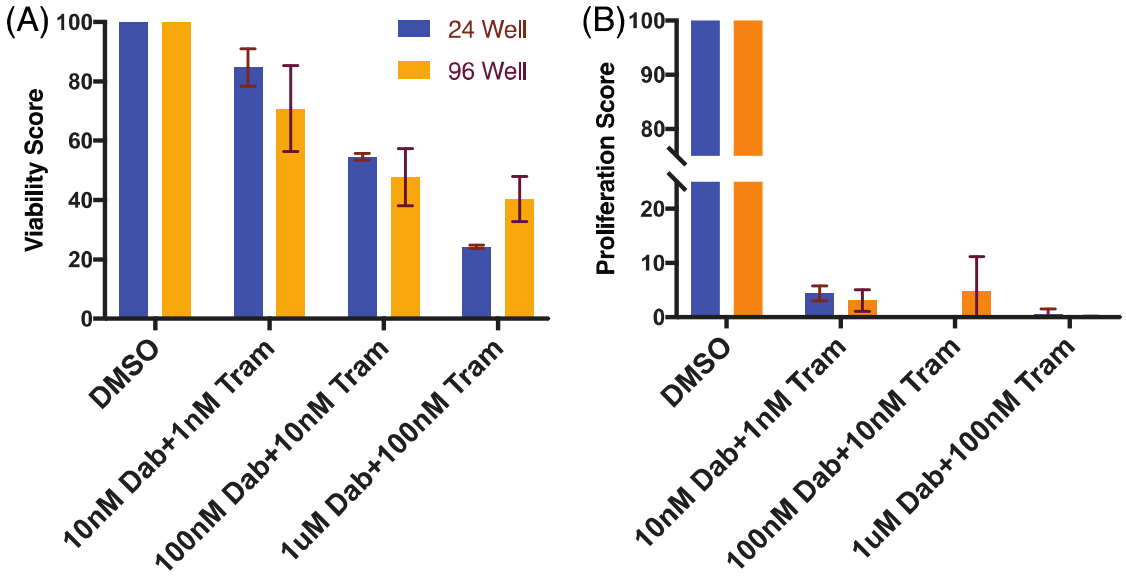

Figure 4: Cells in 3D microenvironment's may be cultured in smaller volumes to reduce cost and increase throughput. A375 melanoma cells cultured in either 24 well or 96 well cell cultures dishes were treated with RMIC as a function of concentration. Viability (A) and proliferation (B) assays were then performed and the results were compared to results acquired from 24 well dishes. No statistical difference was observed. Data represents three independent experimental repeats with results presented as average ± SEM.

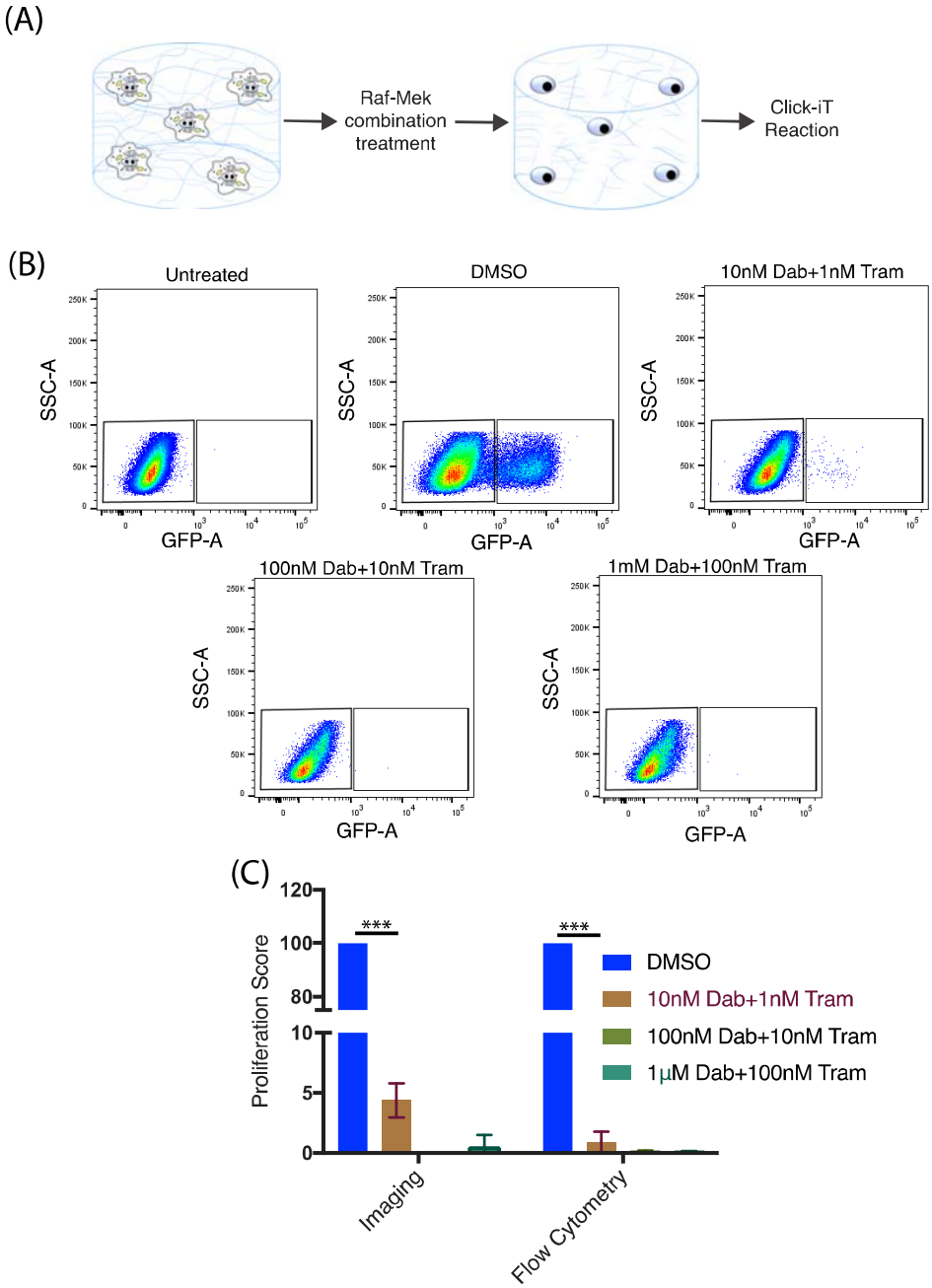

Figure 5: Flow cytometry quantification of proliferation yields similar results to imaging. (A) Cells were cultured and treated in 3D collagen were released from the collagen prior to fluorescence labeling and flow cytometry. Flow cytometry results were gated based on a negative control **(B)** and the results were compared to imaging platform **(C)**. Data represents three independent experimental repeats with results presented as average ± SEM (*** p value < 0.00005).

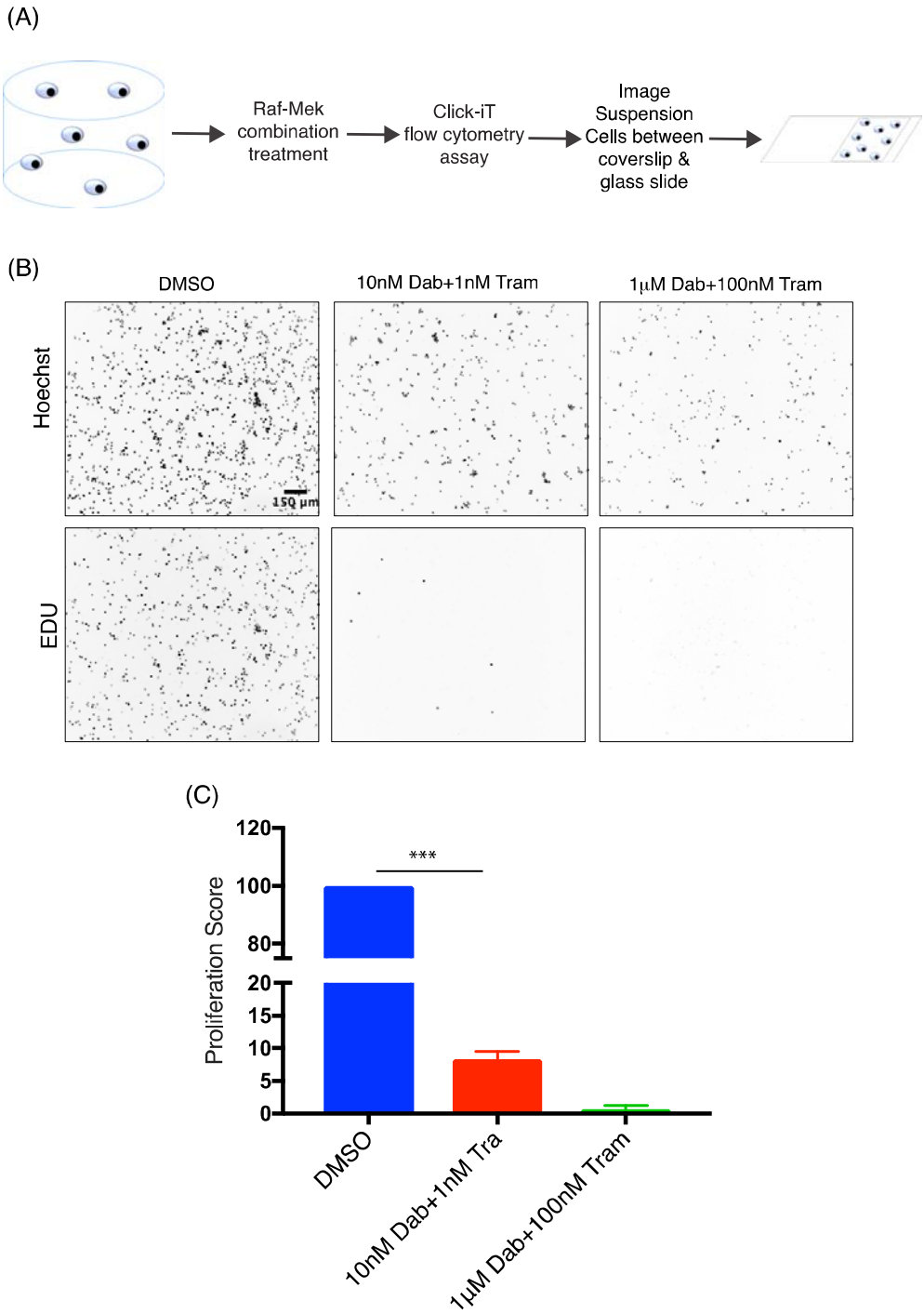

Figure 6: Adaptation of image-based assay to measure cell fate in suspension. (A) Proliferation of A375 cells cultured in suspension was quantified by 2D imaging of cells under a coverslip. **(B)** Example images of suspension cells treated with RMIC. **(C)** Aggregate proliferation scores from three independent experimental repeats reveal proliferation inhibition similar to that observed in cells treated in 3D collagen (p value < 0.00005).

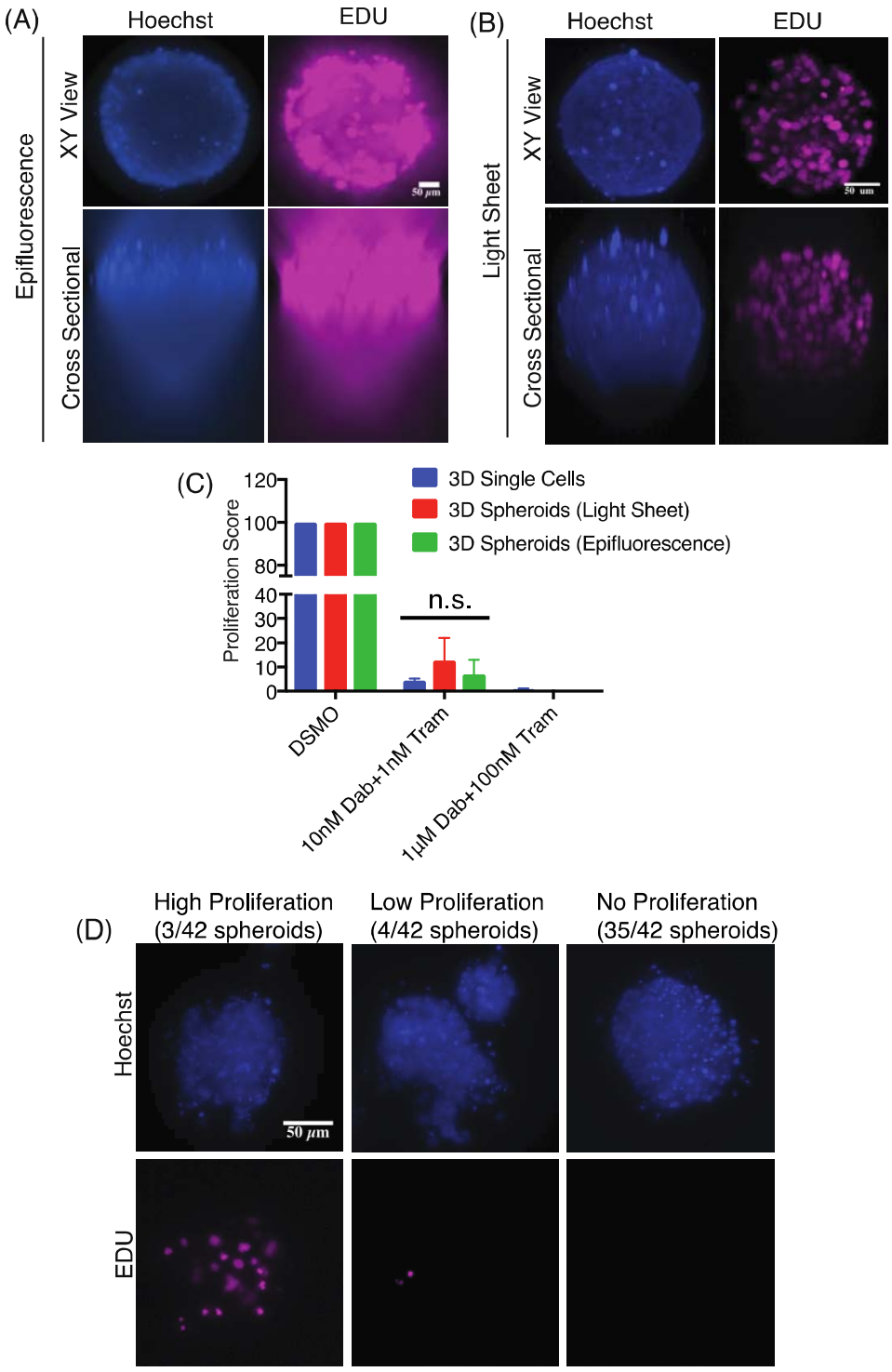

Figure 7: Spheroid models exhibit similar responses to cells in 3D microenvironments while revealing heritable resistance. Example images of A375 melanoma spheroids imaged using wide-field epifluorescence **(A)** compared to LSFM **(B)**. **(C)** Aggregate data comparing the two imaging platforms with similarly treated single cells cultured in 3D collagen. Proliferation score was quantified by normalizing to DMSO control. **(D)** Examples of proliferation heterogeneity in spheroids created from single cells. Of the 42 spheroids imaged 35 showed no proliferation, 4 spheroids showing low proliferation and 3 spheroids showed high proliferation.

1. Holohan C, Van Schaeybroeck S, Longley DB, Johnston PG: **Cancer drug resistance: an evolving paradigm**. *Nature Reviews Cancer* 2013, **13**:714.
2. Maman S, Witz IP: **A history of exploring cancer in context**. *Nature Reviews Cancer* 2018, **18**(6):359-376.
3. Leight JL, Drain AP, Weaver VM: **Extracellular Matrix Remodeling and Stiffening Modulate Tumor Phenotype and Treatment Response**. *Annual Review of Cancer Biology* 2017, **1**(1):313-334.
4. Paszek MJ, Zahir N, Johnson KR, Lakins JN, Rozenberg GI, Gefen A, Reinhart-King CA, Margulies SS, Dembo M, Boettiger D *et al*: **Tensional homeostasis and the malignant phenotype**. *Cancer Cell* 2005, **8**(3):241-254.
5. Wells RG: **The role of matrix stiffness in regulating cell behavior**. *Hepatology* 2008, **47**(4):1394-1400.
6. Edmondson R, Broglie JJ, Adcock AF, Yang L: **Three-Dimensional Cell Culture Systems and Their Applications in Drug Discovery and Cell-Based Biosensors**. *Assay and Drug Development Technologies* 2014, **12**(4):207-218.
7. LaBarbera DV, Reid BG, Yoo BH: **The multicellular tumor spheroid model for high-throughput cancer drug discovery**. *Expert Opinion on Drug Discovery* 2012, **7**(9):819-830.
8. Santo VE, Rebelo SP, Estrada MF, Alves PM, Boghaert E, Brito C: **Drug screening in 3D in vitro tumor models: overcoming current pitfalls of efficacy read-outs**. *Biotechnology Journal* 2017, **12**(1):1600505-n/a.
9. Su Y, Wei W, Robert L, Xue M, Tsoi J, Garcia-Diaz A, Homet Moreno B, Kim J, Ng RH, Lee JW *et al*: **Single-cell analysis resolves the cell state transition and signaling dynamics associated with melanoma drug-induced resistance**. *Proceedings of the National Academy of Sciences* 2017, **114**(52):13679-13684.
10. Shaffer SM, Dunagin MC, Torborg SR, Torre EA, Emert B, Krepler C, Beqiri M, Sproesser K, Brafford PA, Xiao M *et al*: **Rare cell variability and drug-induced reprogramming as a mode of cancer drug resistance**. *Nature* 2017, **546**:431.
11. Tirosh I, Izar B, Prakadan SM, Wadsworth MH, Treacy D, Trombetta JJ, Rotem A, Rodman C, Lian C, Murphy G *et al*: **Dissecting the multicellular ecosystem of metastatic melanoma by single-cell RNA-seq**. *Science (New York, NY)* 2016, **352**(6282):189-196.
12. Long GV, Hauschild A, Santinami M, Atkinson V, Mandalà M, Chiarion-Sileni V, Larkin J, Nyakas M, Dutriaux C, Haydon A *et al*: **Adjuvant Dabrafenib plus Trametinib in Stage III BRAF-Mutated Melanoma**. *New England Journal of Medicine* 2017, **377**(19):1813-1823.
13. Frantz C, Stewart KM, Weaver VM: **The extracellular matrix at a glance**. *Journal of Cell Science* 2010, **123**(24):4195-4200.
14. Theocharis AD, Skandalis SS, Gialeli C, Karamanos NK: **Extracellular matrix structure**. *Advanced Drug Delivery Reviews* 2016, **97**:4-27.
15. Bosman FT, Stamenkovic I: **Preface to extracellular matrix and disease**. *The Journal of Pathology* 2003, **200**(4):421-422.
16. Mouw JK, Ou G, Weaver VM: **Extracellular matrix assembly: a multiscale deconstruction**. *Nature Reviews Molecular Cell Biology* 2014, **15**:771.
17. Quintana E, Shackleton M, Sabel MS, Fullen DR, Johnson TM, Morrison SJ: **Efficient tumour formation by single human melanoma cells**. *Nature* 2008, **456**:593.
18. Welf Erik S, Driscoll Meghan K, Dean Kevin M, Schäfer C, Chu J, Davidson Michael W, Lin Michael Z, Danuser G, Fiolka R: **Quantitative Multiscale Cell Imaging in Controlled 3D Microenvironments**. *Developmental Cell* 2016, **36**(4):462-475.

19. Han YL, Ronceray P, Xu G, Malandrino A, Kamm RD, Lenz M, Broedersz CP, Guo M: **Cell contraction induces long-ranged stress stiffening in the extracellular matrix**. *Proceedings of the National Academy of Sciences* 2018.
20. Hirata E, Girotti Maria R, Viros A, Hooper S, Spencer-Dene B, Matsuda M, Larkin J, Marais R, Sahai E: **Intravital Imaging Reveals How BRAF Inhibition Generates Drug-Tolerant Microenvironments with High Integrin β1/FAK Signaling**. *Cancer Cell* 2015, **27**(4):574-588.
21. Antoni D, Burckel H, Josset E, Noel G: **Three-Dimensional Cell Culture: A Breakthrough in Vivo**. *International Journal of Molecular Sciences* 2015, **16**(3):5517-5527.
22. Friedrich J, Seidel C, Ebner R, Kunz-Schughart LA: **Spheroid-based drug screen: considerations and practical approach**. *Nature Protocols* 2009, **4**:309.
23. Macarron R, Banks MN, Bojanic D, Burns DJ, Cirovic DA, Garyantes T, Green DVS, Hertzberg RP, Janzen WP, Paslay JW *et al*: **Impact of high-throughput screening in biomedical research**. *Nat Rev Drug Discov* 2011, **10**(3):188-195.
24. Workman P, Draetta GF, Schellens JHM, Bernards R: **How Much Longer Will We Put Up With $100,000 Cancer Drugs?** *Cell* 2017, **168**(4):579-583.
25. Hongisto V, Jernström S, Fey V, Mpindi J-P, Kleivi Sahlberg K, Kallioniemi O, Perälä M: **High-Throughput 3D Screening Reveals Differences in Drug Sensitivities between Culture Models of JIMT1 Breast Cancer Cells**. *PLOS ONE* 2013, **8**(10):e77232.
26. Kenny HA, Krausz T, Yamada SD, Lengyel E: **Use of a novel 3D culture model to elucidate the role of mesothelial cells, fibroblasts and extra-cellular matrices on adhesion and invasion of ovarian cancer cells to the omentum**. *International Journal of Cancer* 2007, **121**(7):1463-1472.
27. Kenny HA, Lal-Nag M, White EA, Shen M, Chiang C-Y, Mitra AK, Zhang Y, Curtis M, Schryver EM, Bettis S *et al*: **Quantitative high throughput screening using a primary human three-dimensional organotypic culture predicts in vivo efficacy**. *Nature Communications* 2015, **6**:6220.
28. Mathew B, Schmitz A, Muñoz-Descalzo S, Ansari N, Pampaloni F, Stelzer EHK, Fischer SC: **Robust and automated three-dimensional segmentation of densely packed cell nuclei in different biological specimens with Lines-of-Sight decomposition**. *BMC Bioinformatics* 2015, **16**:187.
29. Packard RRS, Baek KI, Beebe T, Jen N, Ding Y, Shi F, Fei P, Kang BJ, Chen P-H, Gau J *et al*: **Automated Segmentation of Light-Sheet Fluorescent Imaging to Characterize Experimental Doxorubicin-Induced Cardiac Injury and Repair**. *Scientific Reports* 2017, **7**(1):8603.
30. Huisken J, Stainier DYR: **Even fluorescence excitation by multidirectional selective plane illumination microscopy (mSPIM)**. *Optics Letter* 2007, **32**(17):2608-2610.